



Contents lists available at ScienceDirect

Journal of Photochemistry and Photobiology A: Chemistry

journal homepage: www.elsevier.com/locate/jphotochem

Modification of excimer emission of perylene dye thin films by single silver nanocubes

Ryohei Yasukuni^{a,1}, Guillaume Laurent^{a,2}, Kenichi Okazaki^b, Makoto Oki^b,
Tsukasa Torimoto^b, Tsuyoshi Asahi^{a,c,*}

^a Department of Applied Physics, Osaka University, Suita, Osaka 65-0871, Japan

^b Department of Crystalline Materials Science, Graduate School of Engineering, Nagoya University, Nagoya, Aichi 464-8603, Japan

^c Department of Material Science and Biotechnology, Graduate School of Science and Engineering, Ehime University, Matsuyama, Ehime 790-8577, Japan

ARTICLE INFO

Article history:

Available online 23 March 2011

Keywords:

Silver nanoparticle
Single nanoparticle spectroscopy
Excimer emission
Fluorescence enhancement
Spectral shape modulation

ABSTRACT

Modification of the excimer emission of N,N'-bis(2,5-di-tert-butylphenyl)-3,4,9,10-perylene dicarboximide (PDI) by localized surface plasmon resonance (LSPR) of silver nanocubes (SNCs) 100–170 nm in size was investigated by single-particle spectroscopy. SNCs were immobilized on a glass substrate and then covered with a 20-nm-thick PDI film via vacuum vapor deposition. Using fluorescence microscopy to compare areas with and without single SNCs on the same sample, we demonstrated the enhanced intensity and modulated spectral shape of the excimer emission by single SNCs. The excimer emission modification was examined for various sizes of SNCs and different LSPR peak positions, and the electromagnetic field enhancement effect on the radiation emission process was discussed.

© 2011 Elsevier B.V. All rights reserved.

1. Introduction

Over the last few decades, the localized surface plasmon resonance (LSPR) effects of noble metal nanoparticles have attracted considerable research interest. For example, the effect of confining incident light to the near-field gives rise to a highly enhanced electromagnetic field at the particle surface [1]. This enhancement induces new optical phenomena such as surface-enhanced Raman scattering [2–4], fluorescence enhancement [5–10], second-harmonic generation [11] and other nonlinear optical processes [12]. Theoretical and experimental studies [13–15] have demonstrated that particle size and morphology affect the resonance position and the enhancement factor of the electromagnetic field. More precisely, many studies have dealt with the enhancement of dye fluorescence near the nanoparticle surface due to LSPR. A theoretical study by Gersten and Nitzan pointed out the competition between enhancement of fluorescence and energy transfer from the excited dye to the metal particles [16]. Moreover, they found

that the enhancement factor of the dye fluorescence was dependent on numerous parameters including fluorescence quantum yield, distance between the dye and metal particles, and particle characteristics such as size, shape, and aggregation. Experimental studies have since confirmed these theoretical predictions showing highly enhanced fluorescence [17–24]. However, the precise mechanism is still not perfectly understood because LSPR modifies both the excitation and emission processes of the dye. The molecular photoexcitation process is modified due to the large increase in the local electromagnetic field, which then increases the absorption transition probability for molecules near metal particles. It is more complicated for the emission process because LSPR can modify both radiative and non-radiative transitions, which could lead to enhancement or quenching, respectively. Moreover, recent studies emphasize that the excitation wavelength, particle size, and overlap of the LSPR band with the absorption and/or emission spectra of the dye [22–24] are crucial for observing a high enhancement factor of the dye fluorescence.

In this paper, we present the spectral modification of a perylene dye (N,N'-bis(2,5-di-tert-butylphenyl)-3,4,9,10-perylene dicarboximide, PDI) by silver nanocubes (SNCs). In order to see how LSPR modifies the spectroscopic properties of the dye, we built a core-shell structure using an individual SNC as the core and a thin layer of PDI as the shell. Solid-state PDI shows an excimer emission having a large Stokes shift, which allows easy separation of the LSPR enhancement effects on absorption and emission processes [24]. Furthermore, high enhancement of the emission process is

* Corresponding author at: Department of Material Science and Biotechnology, Graduate School of Science and Engineering, Ehime University, Matsuyama, Ehime 790-8577, Japan. Tel.: +81 89 927 9926; fax: +81 89 927 9926.

E-mail address: asahi.tsuyoshi.mh@ehime-u.ac.jp (T. Asahi).

¹ Present address: Organisation et Dynamique des Systèmes, Université Paris 7-Denis Diderot, Paris, France.

² Present address: Laboratoire des Matériaux Mesoscopiques et Nanométriques, Université Pierre et Marie Curie, Paris, France.

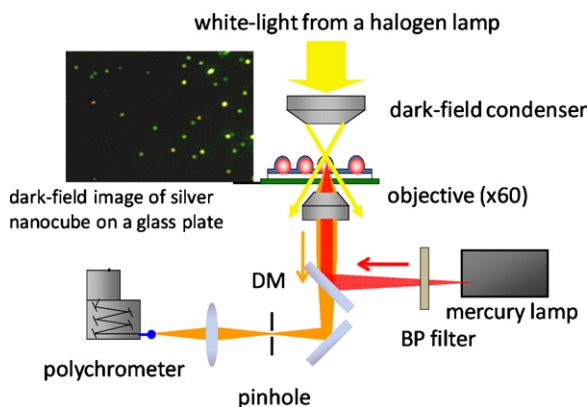


Fig. 1. Light-scattering/fluorescence spectroscopy setup for single-nanoparticle spectroscopy.

expected since excimer emission generally has a small radiative decay constant and small quantum yield. Thus, we observed a large enhancement of the emission intensity by single SNCs. Considering SNCs of various size and different LSPR peak positions, we studied the spectral shape modification in both the fluorescence and its excitation spectrum observation, and we discuss the LSPR enhancement effects on the radiation emission process by SNC.

2. Experimental

2.1. Samples

SNCs were prepared by previously reported synthesis procedures with slight modification [25,26]. The obtained SNCs surface-modified with polyvinylpyrrolidone and having an average edge length of 140 nm were dispersed in ethanol. The solution was spin-coated on a cleaned glass cover slip (Matsunami Industries) and then the SNC-deposited glass substrates were used for single-nanoparticle spectroscopy. We used a diluted SNC solution to ensure sufficient spacing between nanoparticles on the glass substrate; mean spacing was larger than 10 μm , which was confirmed from darkfield optical microscopy images and AFM images. SNCs covered with PDI were prepared by vapor deposition of PDI on SNC-deposited glass substrate using an Ulvac VPC-410 vacuum evaporator (Kiko Inc.). Thickness of the PDI film was typically about 20 nm, determined from AFM and absorption measurements. Absorption spectra for the films were measured using a UV–Vis spectrometer (Shimadzu UV-3100PC).

2.2. Single-particle spectroscopy

Fig. 1 illustrates our light-scattering/fluorescence microscopy setup. The sample on the inverted microscope (IX70, Olympus) was illuminated with white light from a 100-W halogen lamp through a darkfield condenser (U-DCD, Olympus). The scattered light from a single SNC was collected by an objective lens (60 \times , NA 0.7, Olympus) and selected by using an imaging pinhole, and then the spectrum was recorded by a polychromator (77480, Oriel) coupled a liquid-N₂ cooled CCD camera. The fluorescence spectra were measured in the same setup using a high-pressure Hg lamp or the halogen lamp under darkfield configuration as the excitation light source. The excitation wavelength was selected by different optical bandpass filters. By using an imaging pinhole, we could selectively detect the fluorescence from a spatial area of 1.1 μm in diameter.

3. Results and discussion

3.1. Light-scattering spectrum of SNC

To characterize the LSPR band, the light-scattering spectra of single SNCs were measured. We obtained the scattering efficiency spectrum by dividing the detected scattered light intensity of a single nanoparticle by that of a frost plate (DFQ1-30C02-240, Sigma), which showed uniform scattering efficiency in the spectral range of our experimental setup. The scattering efficiency spectra of several single SNCs in air and coated with a PDI film (20-nm thickness) are shown in Fig. 2 as a representative example. The spectra of bare SNCs exhibit two peaks that are characteristic of the LSPR of cubic silver nanoparticles [27,28]. The shorter and longer wavelength peaks correspond to the quadrupole and dipole resonance peak, respectively, and both peaks shifted to longer wavelengths with increasing SNC size [27]. The peak wavelength and scattering efficiency in Fig. 2 show large scatter from particle to particle, which is mainly due to the large distribution in particle size of the SNCs used (see Fig. 3). It can be seen in the SEM image that the edge length ranges from 100 to 170 nm. Comparing the peak distribution in the spectrum measurement with the size distribution in the SEM image, we can roughly evaluate the particle size. For example, a spectrum with peaks at 480 and 650 nm corresponds to an SNC of about 150 nm in edge length.

The single SNCs coated with a PDI thin film show a drastic decrease in light scattering in the wavelength region less than 550 nm, where the PDI film exhibits strong absorption as shown in Fig. 2. Also, a sharp dip was observed at 540 nm. This spectral modulation can be partially attributed to absorption loss of the illuminated light and/or the scattered light by the coated PDI film. It is notable here that the dip position (537 nm) in the scattering spectra is not the same as the absorption peak of the PDI film (530 nm). This observation will indicate coherent coupling between the localized surface plasmon polarization of SNC and the PDI absorption transition dipole [29,30]. The light scattering of SNCs would be dumped by PDI in the wavelength region, leading to the spectral modification of the LSPR scattering. It is known that the coherent coupling is sensitive to the phase difference between the plasmon polarization and molecular transition dipoles. Thus, in the case of gold nanospheres coated with a cyanine J-aggregate, the position of the dip changes with the peak of the LSPR band [29]. However, in the present case of PDI-coated SNCs, the dependence of the dip position was not observed, which will be owing to the broad spectral band of the LSPR.

3.2. Fluorescence modulation

We compared the fluorescence spectra from areas with and without single SNCs on the same sample, and examined the fluorescence modification due to the LSPR. Fig. 4 shows a representative result: the fluorescence intensity is higher with SNCs than without. We calculated the fluorescence modulation spectrum by subtracting the measured fluorescence without SNC from that with SNC, and evaluated the fluorescence intensity enhancement degree (ΔI_F) as the ratio of the fluorescence intensities with and without single SNCs at the emission peak wavelength. As shown in Fig. 5, the values of ΔI_F were higher for single SNCs with larger light-scattering efficiency, i.e. larger-sized SNCs. Because the PDI-coated SNCs samples were prepared by a vacuum deposition, we can safely judge that the number of molecules under the observation area (1.1 μm diameter) is not affected by the presence of SNCs. Alternatively, when we consider a structure where a SNC of a 150-nm edge length coated uniformly with a 20-nm thickness PDI layer, the difference of the number of molecules with and without SNCs was estimated to be less than 10%. The value is smaller than the difference of

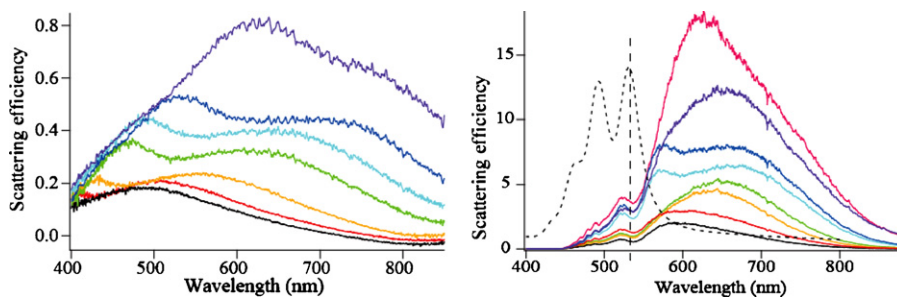


Fig. 2. Light-scattering spectra of single SNCs on a glass substrate (left) and of PDI-covered SNCs (right). Dashed line in right-hand figure: absorption spectrum of a PDI film (20-nm thickness).

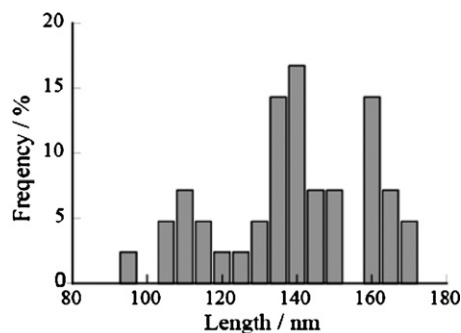
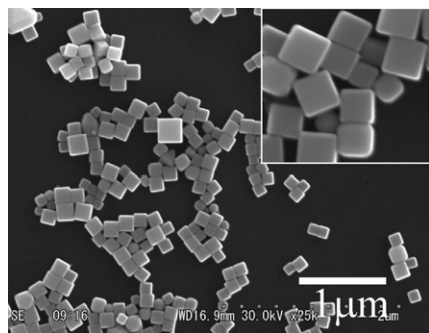


Fig. 3. SEM image of SNCs (left) and distribution of their edge length (right).

the fluorescence intensity with and without SNCs. Therefore, it was concluded that the increase in fluorescence intensity stemmed from PDI molecules near the SNCs.

In order to calculate the enhancement factor, it was necessary to evaluate the exact number of PDI molecules under the enhanced electromagnetic field (near nanoparticles). However, this is difficult to estimate especially in the case of SNCs, because the local field enhancement is highly dependent on the position; significant enhancement takes place only near the edge of the SNC [27,28]. Moreover, studies have shown the importance of the distance

between the metal particles and the dye for observing quenching or enhancement of the fluorescence [18]. Therefore, as described below, we focused on the wavelength dependence of the fluorescence enhancement instead of on the intensity enhancement factor.

Fig. 6 shows the normalized spectra of the fluorescence modulated by three single SNCs and their light-scattering spectra. The peak positions of the enhanced excimer emission differ between the nanoparticles depending on the light-scattering spectrum; an SNC having the scattering peak at a long wavelength exhibits a red-shifted emission peak. We examined about 30 single nanoparticles and summarized the results in Fig. 6. It was observed that the modulated emission peak wavelength increased with the LSPR band peak of the SNC.

Usually, the total fluorescence enhancement factor (EF_{MF}) of a dye molecule is determined by LSPR modification of both the absorption (photoexcitation) and emission processes. It can be evaluated using the following relationship [31]:

$$EF_{MF} \approx \frac{\eta_{abs} \cdot Q_m}{Q_0}, \quad (1)$$

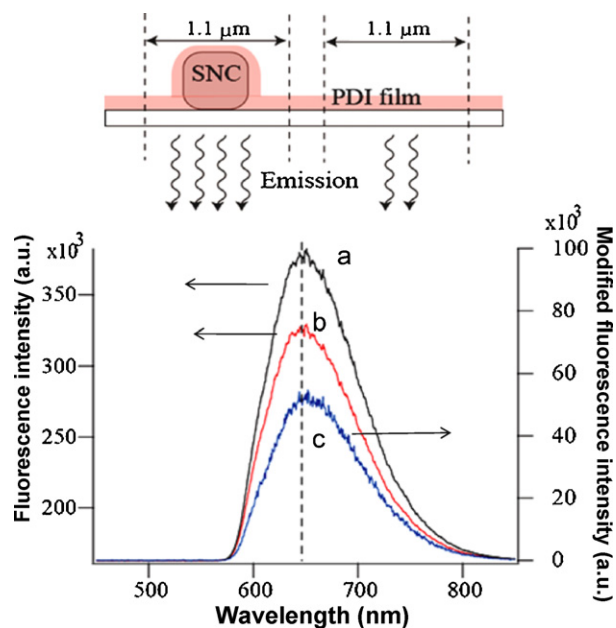


Fig. 4. Simple scheme of the experimental setup with and without SNCs (top). Fluorescence spectra obtained with (a) and without (b) SNCs, and fluorescence modulation spectrum (c) of the PDI dye near the SNCs.

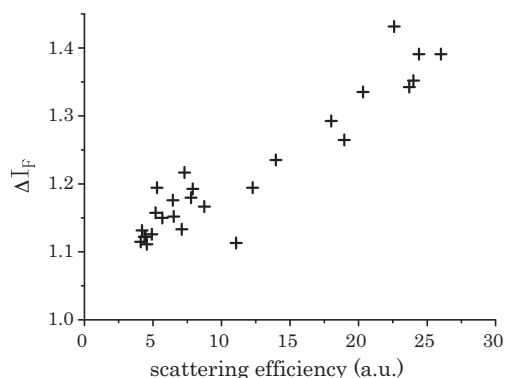


Fig. 5. Relationship between the fluorescence intensity enhancement degree (ΔI_f) and the scattering intensity of single SNCs.

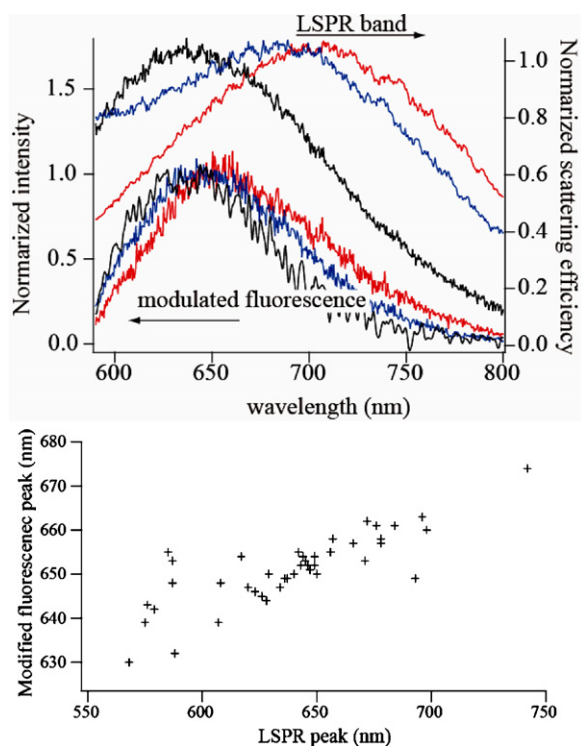


Fig. 6. Spectral shape modulation of excimer emission dependent on the LSPR band of the SNC. The modified emission spectra of PDI near three single SNCs and the light scattering of the corresponding SNCs (top). Relationship between the peak wavelength of the modified emission and the LSPR peak (bottom).

where Q_m and Q_0 refer to the fluorescence quantum yield with and without the metal nanoparticles, respectively. Q_0 is given by $Q_0 = \Gamma / (\Gamma + kn)$, where Γ and kn are the intrinsic radiative emission rate constant and the non-radiative decay rate constant of the excited dye, respectively. $Q_m = \Gamma_m / (\Gamma_m + kn + kq)$, where Γ_m and kq mean enhanced radiative emission rate by LSPR and fluorescence quenching rate by the nanoparticle. Eq. (1) can be written as

$$EF_{MF} \approx \frac{\eta_{abs} \cdot (\Gamma_m / \Gamma)}{[(\Gamma + kn) / (\Gamma_m + kn + kq)]}. \quad (2)$$

The local field E_{Loc} (present at the molecule position) is modified compared to the incident local field E_0 by a local field enhancement factor, EF. The photoexcitation enhancement factor (η_{abs}) at the angular frequency of the excitation light (ω_{ex}) can be roughly estimated by the following relationship:

$$\eta_{abs}(\omega_{ex}) \approx EF(\omega_{ex}) = \frac{|E_{Loc}(\omega_{ex})|^2}{|E_0(\omega_{ex})|^2}. \quad (3)$$

The field enhancement of the radiative emission processes can be linked to EF using the optical reciprocity theorem [32]. It can be considered in the first approximation that the radiative emission enhancement factor ($EF_{RM} = \Gamma_m / \Gamma$) and EF are of the same order of magnitude at the frequency of the emission light (ω_f), i.e.:

$$EF_{RM}(\omega_f) = \Gamma_m / \Gamma \approx EF(\omega_f). \quad (4)$$

Therefore, Eq. (2) can be rewritten as

$$EF_{MF} \approx \eta_{abs}(\omega_{ex}) \cdot EF_{RM}(\omega_f) \cdot \left(\frac{\tau_m}{\tau_0} \right), \quad (5)$$

where τ_0 and τ_m mean the fluorescence lifetime with and without the metal nanoparticles, respectively. Since $\tau_0 = 1 / (\Gamma + kn)$ and $\tau_m = 1 / (\Gamma_m + kn + kq)$, the value of τ_m / τ_0 is smaller than 1. Namely, this term in Eq. (5) means the suppression of the fluorescence enhancement. On the other hand, the large values of η_{abs} and EF_{RM}

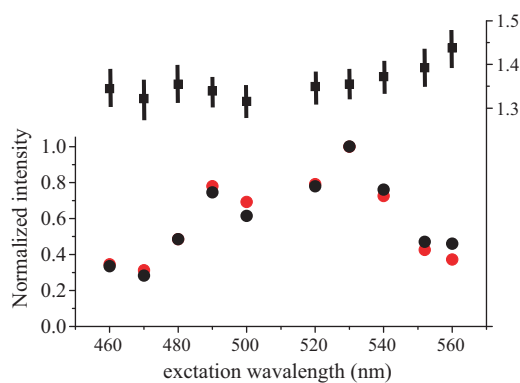


Fig. 7. Excitation spectra for PDI dye near SNC (black filled circle) and in dye thin film (red one), and excitation wavelength dependence of the emission enhancement factor (black square). (For interpretation of the references to color in this figure legend, the reader is referred to the web version of the article.)

can be expected when the LSPR band overlaps with the absorption and fluorescence bands of a dye molecule. In the present case of SNC-PDI hybrid films, both the absorption and emission bands of PDI overlap the LSPR of SNC, as shown in Figs. 2 and 4. Therefore, we cannot conclude whether the LSPR modifications of the excitation and emission processes are dominant in EF_{MF} , as far as considering the enhancement of the total fluorescence intensity.

An important aspect of Eq. (5) is the frequency (wavelength) dependence of EF_{MF} . If we assume that EF has a similar frequency dependence on the LSPR band, the value of $EF_{RM}(\omega_f)$ becomes large at wavelengths close to the peak of the LSPR band. This consideration predicts the spectral shape modulation of the enhanced fluorescence by SNC, and it agrees with the experimental observation in Fig. 6. Therefore, we can consider that electromagnetic field enhancement of the radiative emission rate occurs in the present system of SNCs covered with a PDI thin film. Most studies on fluorescence modification by LSPR deal with the intensity enhancement factor of the dye fluorescence, but few studies concentrate on the modification of the shape of the emission spectra. Le Ru et al. recently reported that the emission from the Franck-Condon excited state (vibrationally unrelaxed excited states) of dyes adsorbed on silver nanoparticles exhibits a large spectral shape modulation, and that the spectral profile is affected by relaxation dynamics in the excited state [31]. However, the present work indicates that the fluorescence spectral shape of the relaxed excited state can be modified by the LSPR.

On the other hand, Eq. (5) demonstrates the wavelength dependence of the photoexcitation modulation by LSPR. We examined the excitation spectrum of the modulation emission by SNC and compared it to that of the PDI film without SNCs. The intensity of the modulated emission at various excitation wavelengths were measured for the same single SNC and the dependence was plotted in Fig. 7. To check photodegradation of the sample, we compared the emission intensities before and after the measurement, and confirmed that the difference of the intensity was less than 3%. The wavelength dependence was the similar to that of the PDI film, while the fluorescence intensity enhancement degree, ΔI_f , was slightly dependent on the excitation wavelength. The values became large at wavelengths longer than 520 nm, which suggests that the photoexcitation process is also enhanced by the LSPR of SNC.

4. Conclusions

In conclusion, the modification of the excimer emission of PDI thin films by single SNCs of 100–170 nm in size was demonstrated by single-nanoparticle fluorescence/light scattering microspectrum.

troscopy. We observed the intensity enhancement as well as spectral shape modification of PDI emission near SNC dependent on the LSPR band peak position. The modulated emission peak wavelength increased with the LSPR band peak, indicating to the electromagnetic field enhancement of the radiative transition rate of the excimer emission. This work ensures that the fluorescence spectral shape of relaxed excited states can be modified by the LSPR.

Acknowledgement

This work was partly supported by a Grant-in-Aid for Scientific Research on Priority Area “Strong Photon-Molecule Coupling Fields” (No. 470) from the Ministry of Education, Culture, Sports, Science and Technology of Japan.

References

- [1] H. Raether, Surface plasmons on smooth and rough surfaces and on gratings, in: G. Hühler (Ed.), Springer Tracts in Modern Physics, vol. 111, Springer, Berlin, 1988.
- [2] P.F. Liao, J.G. Bergman, D.S. Chemla, A. Wokaun, J. Mengalis, A.M. Hawryluk, N.P. Economou, Chem. Phys. Lett. 82 (1981) 355.
- [3] L. Gunnarsson, E.J. Bjerneld, H. Xu, S. Petronia, B. Kaserno, M. Kahl, Appl. Phys. Lett. 78 (2001) 802.
- [4] G. Laurent, N. Félidj, S. Lau Truong, J. Aubard, G. Lévi, J.R. Krenn, A. Hohenau, A. Leitner, F.R. Aussenegg, Nano Lett. 5 (2005) 253.
- [5] A. Wokaun, H.P. Lutz, A.P. King, U.P. Wild, R.R. Ernst, J. Chem. Phys. 79 (1983) 509.
- [6] D.A. Weitz, S. Garoff, J.I. Gersten, A. Nitzan, J. Chem. Phys. 78 (1983) 5324.
- [7] J.R. Lacowicz, Y. Shen, S. D'Auria, J. Malicka, J. Fang, Z. Gryczynski, I. Gryczynski, Anal. Biochem. 301 (2002) 261.
- [8] J.R. Lacowicz, Anal. Biochem. 337 (2005) 171.
- [9] J. Zhang, J.R. Lacowicz, Opt. Exp. 15 (2007) 2598.
- [10] E. Fort, S. Grésillon, J. Phys. D: Appl. Phys. 41 (2008) 013001.
- [11] K. Tsuboi, K. Seki, Y. Ouchi, K. Fujita, K. Kajikawa, Jpn. J. Appl. Phys. 42 (2003) 607.
- [12] Y. Hamanaka, K. Fukuta, A. Nakamura, L.M. Liz-Marzan, P. Mulvaney, Appl. Phys. Lett. 84 (2004) 4938.
- [13] U. Kreibitz, M. Volmer, Optical Properties of Metal Clusters, Springer, Berlin, 1995.
- [14] D.S. Wang, M. Kerker, Phys. Rev. B 24 (1981) 1777.
- [15] P.W. Barber, R.K. Chang, H. Massoudi, Phys. Rev. Lett. 50 (1983) 997.
- [16] J. Gersten, A. Nitzan, J. Chem. Phys. 75 (1981) 1139.
- [17] T. Nakamura, S. Hayashi, Jpn. J. Appl. Phys. 44 (2005) 6833.
- [18] P. Anger, P. Bharadwaj, L. Novotny, Phys. Rev. Lett. 96 (2006) 113002.
- [19] Y. Zhang, K. Aslan, J.R. Previte, C.D. Geddes, Appl. Phys. Lett. 90 (2007) 053107.
- [20] S. Kühn, U. Hakanson, L. Rogobete, V. Sandoghdar, Phys. Rev. Lett. 97 (2006) 017402.
- [21] M. Thomas, J.J. Greffet, R. Carminati, J.R. Arias-Gonzales, App. Phys. Lett. 85 (2004) 3863.
- [22] F. Tam, G.P. Goodrich, R.B. Johnson, N.J. Halas, Nano Lett. 7 (2007) 496.
- [23] Y. Chen, K. Munechika, D.S. Ginger, Nano Lett. 7 (2007) 690.
- [24] G. Laurent, T. Asahi, Chem Lett. 111 (2007) 1549.
- [25] Y.G. Sun, Y.N. Xia, Science 298 (2002) 2176; P. Bharadwaj, P. Anger, L. Novotny, Nanotechnology 18 (2007) 044017.
- [26] K. Okazaki, J. Yasui, T. Torimoto, Chem. Commun. (2009) 2917.
- [27] J.M. McMahon, Y. Wang, L.J. Sherry, R.P. Van Duyne, L.D. Marks, S.K. Gray, G.C. Schatz, J. Phys. Chem. C 113 (2009) 2731.
- [28] F. Zhou, Z.-Y. Li, Y. Liu, Y. Xia, J. Phys. Chem. C 112 (2008) 20233.
- [29] T. Uwada, R. Toyota, H. Masuhara, T. Asahi, J. Phys. Chem. C 111 (2007) 1549.
- [30] G.P. Wiederrecht, G.A. Wurtz, J. Hranisavljevic, Nano Lett. 4 (2004) 2121.
- [31] E.C. Le Ru, P.G. Etchegoin, J. Grand, N. Félidj, J. Aubard, G. Lévi, J. Phys. Chem. C 111 (2007) 16076.
- [32] E.C. Le Ru, P.G. Etchegoin, Chem. Phys. Lett. 423 (2006) 63.